

# Hydrogels with Preprogrammable Lifetime via UV-Induced Polymerization and Degradation

Johannes M. Scheiger and Pavel A. Levkin\*

Hydrogels are 3D networks infused with water. When formed via radical polymerization, inherently stable hydrogels are created due to stable covalent carbon-carbon bonds. As such, they remain static soft scaffolds, unlike the dynamic tissue they are often compared to. Herein, a hydrogel capable of autonomously converting from a liquid hydrogel precursor solution into a solid hydrogel for a defined period of time, followed by a further transformation back into a liquid polymer solution, is designed. These antagonistic processes are initiated by the same UV light, which is used as stimulus for both a photopolymerization and a photodegradation simultaneously. It is demonstrated how the lifetime of the hydrogel state can be controlled and visualized on the minute scale. Both the photopolymerization and the photodegradation reactions are studied with various methods such as NMR, IR, and confocal microscopy. The different stages of the transformation, e.g., the hydrogel precursor (liquid), hydrogel (solid), and degraded hydrogel (liquid) are investigated with rheometry, viscosimetry, dynamic light scattering, and gel permeation chromatography. Small changes in the molecular composition of the precursor solution result in macroscopically measurable differences. Such time-dependent twofold photoreactive systems can be of interest for designing dynamic materials, such as glues and photoresists or for biomedical applications.

## 1. Introduction

Polymer chemistry has developed from uncontrolled radical polymerizations to reactions with remarkable control of products in terms of molar mass,<sup>[1]</sup> polydispersity, polymer conformation (e.g., folding of single polymer chains),<sup>[2]</sup> tacticity, sequence control,<sup>[3]</sup> and polymer architecture.<sup>[4,5]</sup> With controlled radical polymerization techniques such as ATRP

(atom transfer radical polymerization), RAFT (reversible addition-fragmentation chain transfer polymerization) or NMP (nitroxide-mediated polymerization), polymers can be tailored to suit the respective needs of application. Despite the enormous progress in radical polymerizations, control over the lifetime of polymers remains a challenge due to the strong covalent carbon-carbon bonds formed. Controllably induced gelation and liquefaction processes are sought particularly for hydrogels due to their applications in drug release or 3D cell culture.<sup>[6-8]</sup> Recently, a group of smart “non-equilibrium” or “autonomous” materials allowed predefining the lifetime of supramolecular hydrogels.<sup>[9-11]</sup> Since then, a few strategies have been exploited to preprogram the lifetime of supramolecular hydrogels, making use of either antagonistic enzymes,<sup>[10-14]</sup> kinetically competing reactions,<sup>[15]</sup> or the generation of thermodynamically unfavorable molecules which self-assemble into hydrogels.

Formation of latter are fueled by molecules high in energy (e.g., carbodiimides or dimethylsulfate).<sup>[10,16,17]</sup> Hydrogels with predefined lifetime have been limited to supramolecules and one example of an anhydride crosslinked acryl amide/acrylic acid copolymer.<sup>[18]</sup> Moreover, hydrogels formed and crosslinked via radical polymerizations cannot be addressed by existing strategies.

Permanent covalent hydrogels are fundamentally different from supramolecular hydrogels: while the latter form networks due to self-assembly, covalent hydrogels are formed via polymerization of monomers with crosslinkers.<sup>[19-21]</sup> The stability of covalent bonds results in a higher chemical resistance, higher thermal and thermodynamic stability as well as tunable mechanical properties. Herein, we report the ability to control the lifetime of a covalently crosslinked hydrogel by combining an UV-induced photopolymerization with an UV-induced photodegradation. This process is driven by a single UV light source, thus rendering the process of formation and degradation autonomous, i.e., if the UV light is applied continuously, a hydrogel precursor solution starts a transition from liquid into solid and then, after a defined period of time, to liquid again. For the first time, control over a covalently crosslinked hydrogel is demonstrated not only spatially but also temporally, thus rendering the UV-induced formation and degradation of hydrogels (UV transient hydrogels) an example for 4D macromolecular engineering.

J. M. Scheiger, Dr. P. A. Levkin  
Institute of Biological and Chemical Systems (IBCS-FMS)  
Karlsruhe Institute of Technology (KIT)  
Hermann-von-Helmholtz Pl. 1 76344, Eggenstein-Leopoldshafen,  
Germany  
E-mail: levkin@kit.edu

J. M. Scheiger, Dr. P. A. Levkin  
Institute of Organic Chemistry (IOC)  
Karlsruhe Institute of Technology (KIT)  
76021, Karlsruhe, Germany

 The ORCID identification number(s) for the author(s) of this article can be found under <https://doi.org/10.1002/adfm.201909800>.

© 2020 The Authors. Published by WILEY-VCH Verlag GmbH & Co. KGaA, Weinheim. This is an open access article under the terms of the Creative Commons Attribution-NonCommercial License, which permits use, distribution and reproduction in any medium, provided the original work is properly cited and is not used for commercial purposes.

DOI: 10.1002/adfm.201909800

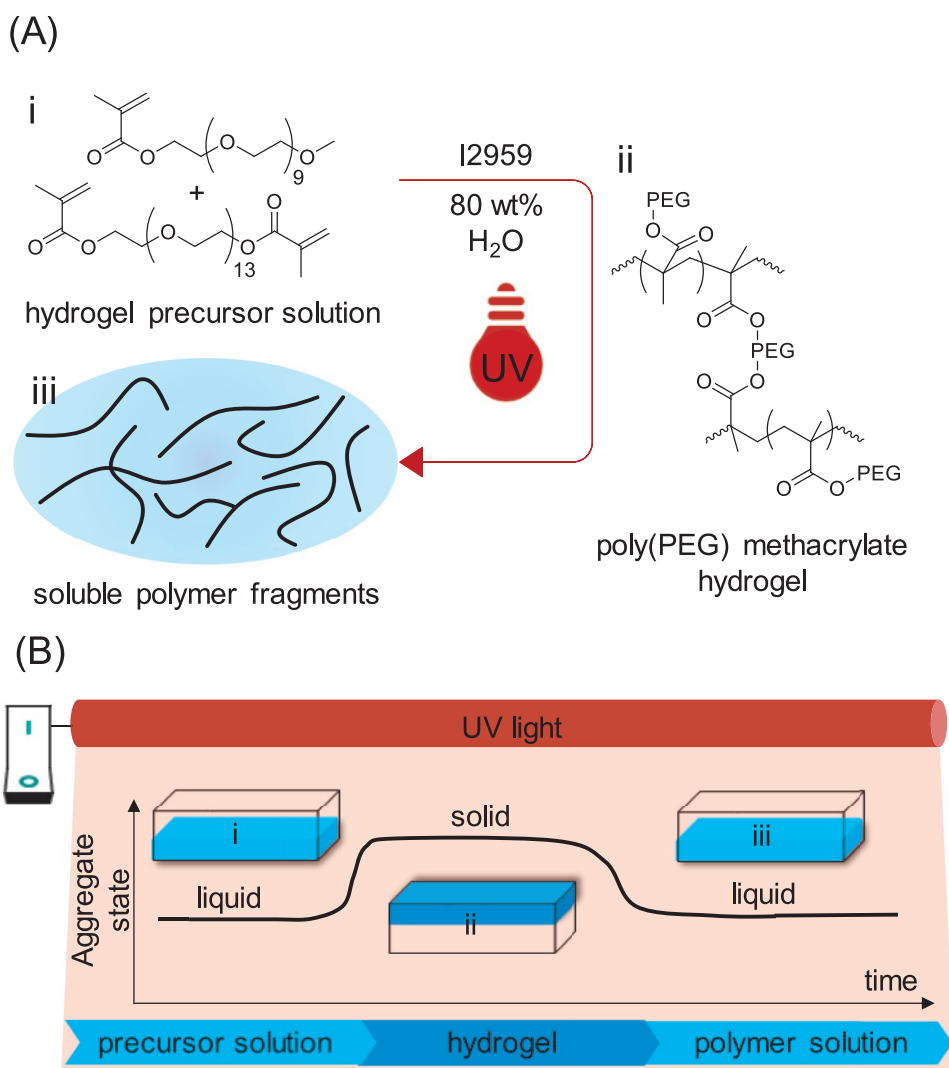


**Figure 1.** A) Reaction equation and B) schematic showing the UV-induced preprogrammed formation and degradation of a hydrogel. UV irradiation of a hydrogel precursor solution (i) induces rapid polymerization, resulting in a solid hydrogel state (ii). Further continuous UV irradiation degrades the hydrogel into a polymer solution (iii). Since the photodegradation kinetics are slower than those of the photopolymerization, the lifetime of the solid hydrogel state is finite and can be preprogrammed by fine-tuning the precursor solution composition and UV-light intensity.

## 2. Results and Discussion

In all transient macromolecular materials with definable lifetime, building blocks are incorporated into molecules of higher order (e.g., a hydrogel network), which undergo degradation either simultaneously with their formation or timely delayed via a feedback mechanism. Here we report on UV transient hydrogels, which principle is shown in **Figure 1A,B**. In all experiments, poly(ethylene glycol) methylether methacrylate (PEGMA, MW 500) monomers were copolymerized with the crosslinker poly(ethylene glycol) dimethacrylate (PEGDMA, MW 750) in a ratio of PEGMA-PEGDMA-*X*, with *X* being  $\frac{n_{\text{PEGMA}}}{n_{\text{PEGMA}} + n_{\text{PEGDMA}}}$ . The water content of the precursor

solution was 80 wt% (relative to PEGMA). As photoinitiator 0.005 mol% (rel. to PEGMA) 2-hydroxy-4'-(2-hydroxyethoxy)-2-methylpropiophenone (I2959) was used. The UV light sources

employed were Hg-lamps with similar light emission peaks (Figures S1–S3, Supporting Information) but different power (termed “weak” and “strong”). More detailed information about the choice of reactants and composition of the hydrogel precursor solution can be found in the Supporting Information.

For a typical experimental setup, the prepolymer mixture was irradiated with UV light (4 mW cm<sup>−2</sup> at 260 nm), triggering formation of a “solid” hydrogel within a few minutes (**Figure 2Ai** → ii). However, continuation of the UV irradiation of the hydrogel led to the transformation of the hydrogel into a liquid solution (**Figure 2Aii** → iii). The same UV light initiating the polymerization simultaneously caused degradation of the covalent polymethacrylate network into water soluble polymer fragments, effectively converting the hydrogel into an aqueous polymer solution. Due to the inherent stability of covalent hydrogels, the process could be stopped at any desired time, simply by preventing the hydrogel from further UV light

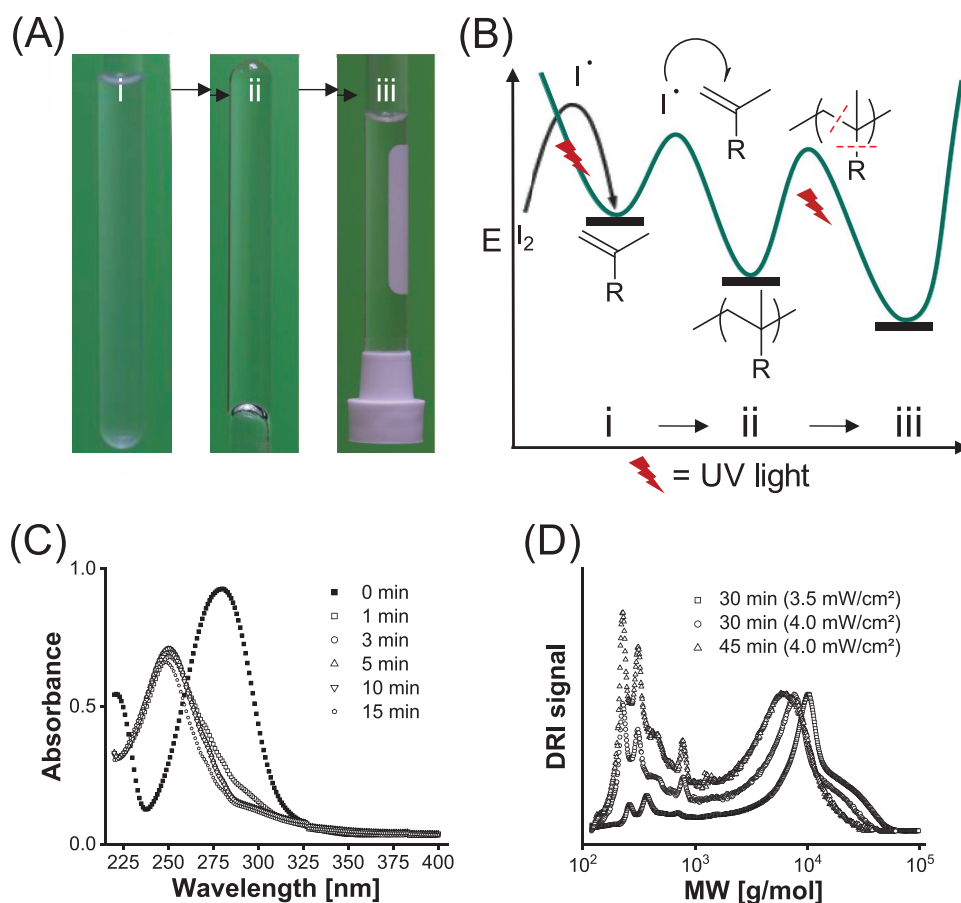


**Figure 2.** A) Process of UV-induced formation and degradation of a PEGMA-PEGDMA-5 hydrogel. Pictures were taken after 0 min (i), 20 min (ii) and 120 min (iii) of UV irradiation of 500  $\mu\text{L}$  PEGMA-PEGDMA-5 precursor solution in a UV transparent NMR tube. B) Reaction-energy diagram for the UV-induced formation and degradation of PEGMA-PEGDMA hydrogels. UV light provides the activation energy for the cleavage of photoinitiator molecules leading to polymerization, as well as for the cleavage of the polymeric network, leading to hydrogel degradation. The driving force of the polymerization is the conversion of carbon–carbon double to single bonds. R represents either the  $(\text{CO}_2)\text{-PEG-OMe}$  unit of PEGMA or the  $(\text{CO}_2)\text{-PEG-(CO}_2\text{C}_3\text{H}_5)$  unit of PEGDMA. C) UV spectra of the photoinitiator Irgacure 2959 in water after exposure to UV irradiation for different times. The maximum shifted almost completely after only 1 min, indicating an efficient generation of radicals and fast polymerization. D) Influence of the UV irradiation time on the molecular weight distribution (MWD) of a PEGMA-PEGDMA-5 hydrogel as determined with gel permeation chromatography (GPC). Hydrogel discs were irradiated with UV light for different times until fully liquefied samples were obtained. The MWD shifts to lower molecular masses and high MW shoulders disappear upon UV irradiation.

exposure (Figure 2A). This approach differs fundamentally from all transient hydrogels reported so far, due to its different gelation and degradation mechanisms, driving forces, stimulus, network type, and energetic landscape (Figure 2B, Table S1, Supporting Information). The polymerization reaction itself is fueled by the exothermic conversion of methacrylic carbon–carbon double bonds into single bonds ( $\approx 54 \text{ kJ mol}^{-1}$  for methyl methacrylate), which easily overcomes the activation energy of propagation ( $\approx 20 \text{ kJ mol}^{-1}$  for the PEGMA used in this report).<sup>[22,23]</sup> Without further irradiation, the hydrogel state would resemble a stable energetic minimum but the continuous UV irradiation cleaves carbon–carbon bonds in the polymer and thus guides the system into a consecutive energy minimum (Figure 2B). Mechanistically, random main-chain scission or main-chain scission induced by side chain scission can occur (or both), leading to a broad mixture of possible products.<sup>[24–32]</sup> It is thus hard to determine the exact position of the degraded hydrogel state in the energetic landscape. However,

the energy level of the degraded polymer solution could be lower than that of the hydrogel due to the formation of stable C–H bonds as in formates, which were identified by NMR spectroscopy (Figure S4, Supporting Information).

UV light drives such antagonistic processes because it provides the activation energy required for two processes (Figure 2B): The cleavage of the photoinitiator, thus initiating a free radical polymerization (i  $\rightarrow$  ii) and also the energy necessary to cleave the polymeric network into soluble polymer fragments, leading to re-liquefaction (ii  $\rightarrow$  iii). These two processes happen on different time scales, i.e., the polymerization is faster than the degradation, and the systems undergo a transformation from a liquid precursor to a hydrogel state, followed by a transition into a degraded hydrogel polymer solution. The fast polymerization was attributed to the efficient cleavage of photoinitiator molecules (Figure 2C). In a model experiment, we irradiated a solution of the photoinitiator I2959 in water for different times ( $4 \text{ mW cm}^{-2}$ ). The concentration used was equal to

the one used for the polymerization ( $0.2 \text{ mmol L}^{-1}$ ). Within just 1 min the absorbance maximum shifted from 280 to 250 nm. Interestingly, an almost exactly opposite shift (from 247 to 279 nm) was reported recently in a photopolymerization study using I2959.<sup>[33]</sup> This could be caused by the different solvent PBS (phosphate buffered saline) and the different irradiation conditions (365 nm) used in this study. An in-depth report about the photocleavage mechanism of I2959 is in accordance with our value of the absorption maximum of aqueous I2959 solution being at 280 nm.<sup>[34]</sup> The model system is believed to behave similar to the polymerization mixture, since the main absorbance of I2959 around 280 nm was found to be uncontested by the monomer PEGMA and crosslinker PEGDMA, respectively (Figure S5, Supporting Information). Oppositely, the photodegradation was a slow process, where only extended periods of irradiation time had a measurable effect. Long time UV irradiation (30 min) of swelled PEGMA-PEGDMA-5 hydrogel led to full liquefaction into an aqueous solution, which could then be dried and examined with gel permeation chromatography (GPC, Figure 2D). For increasing irradiation times and UV intensity (30 min at  $3.5 \text{ mW cm}^{-2}$ , 30 min and 45 min at  $4.0 \text{ mW cm}^{-2}$ ), a decrease in all molecular weight distribution (MWD) parameters ( $M_p$ ,  $M_n$ ,  $M_w$ ) was observed (Table S2, Supporting Information). Noteworthy, the MWD parameters extracted are not representative for the whole elugram, as the respective MWDs outspread to very low molecular weights ( $<M_w 800$ ), where the GPC calibration used is not valid anymore. Therefore, only the parts of the elugrams corresponding to masses greater than 800 Da were integrated. The broad shoulder after 30 min irradiation (seen for both  $3.5$  and  $4.0 \text{ mW cm}^{-2}$ ) of the MWD disappeared after 45 min of UV irradiation, which indicated an unselective (random) degradation mechanism. High molecular weight polymer chains are statistically more likely to undergo chain scission than low molecular weight chains due to the presence of more cleavable bonds per polymer. Polymer chains also have a higher statistical probability to be cleaved in the middle of the chain rather than at the chain ends contributing to the disappearance of the high molecular weight shoulder. This assumption was further supported by a decrease in the polydispersity  $\mathcal{D}$  with increasing irradiation time (Table S2, Supporting Information).

The inherent lifetime of the hydrogel state depends on both the UV irradiation conditions and on the composition of the precursor solution, which could be adjusted to prolong or shorten the hydrogels lifetime. To illustrate the influence of irradiation time and intensity on the gelation and degradation, we prepared hydrogel precursor solution films in between a glass slide and a quartz slide (on top), separated by a spacer ( $125 \mu\text{m}$ ). The hydrogel films were then irradiated with two different UV lamps (“weak” and “strong”) for different times. After irradiation, films of PEGMA-PEGDMA-5 precursor solution were swelled in aqueous Rhodamine-110 Cl ( $5 \text{ mg L}^{-1}$ ) solution and then imaged with confocal laser scanning microscopy (CLSM) (Figure 3A). Due to the swelling in aqueous Rhodamine-110 Cl solution ( $5 \text{ mg L}^{-1}$ ), hydrogel films increased in height from 125 to  $\approx 450 \mu\text{m}$ . Hydrogel film formation was observed after 1 and 2 min for the strong and weak UV lamp, respectively. The photodegradation clearly showed to be a surface erosion process, which allowed illustration of the lifetime of UV transient hydrogels as

a function of height versus irradiation time. The hydrogel film thickness was at its maximum right after its formation, because the UV photodegradation took place simultaneously. Thereafter, a monotonous decrease in hydrogel height was observed with increasing irradiation time. When using a strong UV light source ( $1000 \text{ W}$ ), both the polymerization as well as the photodegradation were faster than in the case of using a weak UV light source ( $500 \text{ W}$ ), i.e., the gelation and degradation time were 1 min and 21 min shorter, respectively. Thus, the lifetime of UV transient hydrogels could be adjusted via the UV light intensity. Noteworthy, the use of a filter blocking UV light below 320 nm slowed down the polymerization (no quantitative conversion of vinyl groups after 20 min) and did not lead to observable degradation (Figure S6, Supporting Information).

Compared to our previous report, the photodegradation rate is  $\approx 10$ -fold slower in terms of photodegradation depth per time ( $\mu\text{m min}^{-1}$ ).<sup>[35]</sup> This is attributed to the fact that the UV transient hydrogels in this work were not allowed to reach their maximum water swelling level, which would accelerate their degradation. The swelling ratio for PEGDMA-PEGDMA-5 hydrogels was calculated from the weight of as-prepared hydrogels and swelled hydrogels. Gels could take up DI water  $4.25 \pm 0.15$  times their own network weight, respectively. Another reason for the slow photodegradation could be the presence of UV absorbing photoinitiator molecules.

To gain insight into the polymerization reaction, i.e., the monomer and photoinitiator conversion, UV transient hydrogel films were examined with FTIR ATR and in situ UV spectroscopy with a radial spectrophotometer. In the ATR FTIR (attenuated total reflection Fourier transform infrared spectroscopy) spectra recorded for different irradiation times, PEGMA and PEGDMA double bond conversion could not be observed from the double bond stretching band at  $1640 \text{ cm}^{-1}$ , as it was overlaid by the very broad and intense water bending band peaking around  $1635 \text{ cm}^{-1}$ . Instead, the shift from the  $\alpha$ - $\beta$  unsaturated ester stretching band in the monomer ( $1716 \text{ cm}^{-1}$ ) to a saturated, aliphatic ester stretching band ( $1727 \text{ cm}^{-1}$ ) in the converted polymethacrylate network was observed (Figure 3B). After 5 min irradiation, there was no more observable change upon further irradiation, indicating that the polymerization reaction was completed after this time (full spectra Figure S7, Supporting Information). PEGMA-PEGDMA-5 precursor solution films irradiated for 2, 3, 4, and 5 min yielded smooth gel films. Films irradiated for longer times already showed signs of degradation visible with the bare eye by the formation of droplets on the gel surface, indicating that the leftover gel film could not take up all the water freed due to the network degradation. Since formation of PEGMA-PEGDMA-5 hydrogel films was observed already after 2 min by CLSM, it was concluded that gelation of PEGMA-PEGDMA-5 precursor solution did not require quantitative monomer conversion.

UV-vis spectroscopy has shown to be a useful complementary technique to infrared spectroscopy for the investigation of monomer and photoinitiator conversion.<sup>[36,37]</sup> Hence, we investigated the consumption of the photoinitiator via in situ UV spectroscopy, using a spectral radiophotometer (Figure 3C). A hydrogel precursor film ( $125 \mu\text{m}$ ) in between two quartz glass slides was placed on top of the sensor of the spectral radiophotometer, which was put underneath the UV lamp. Every minute

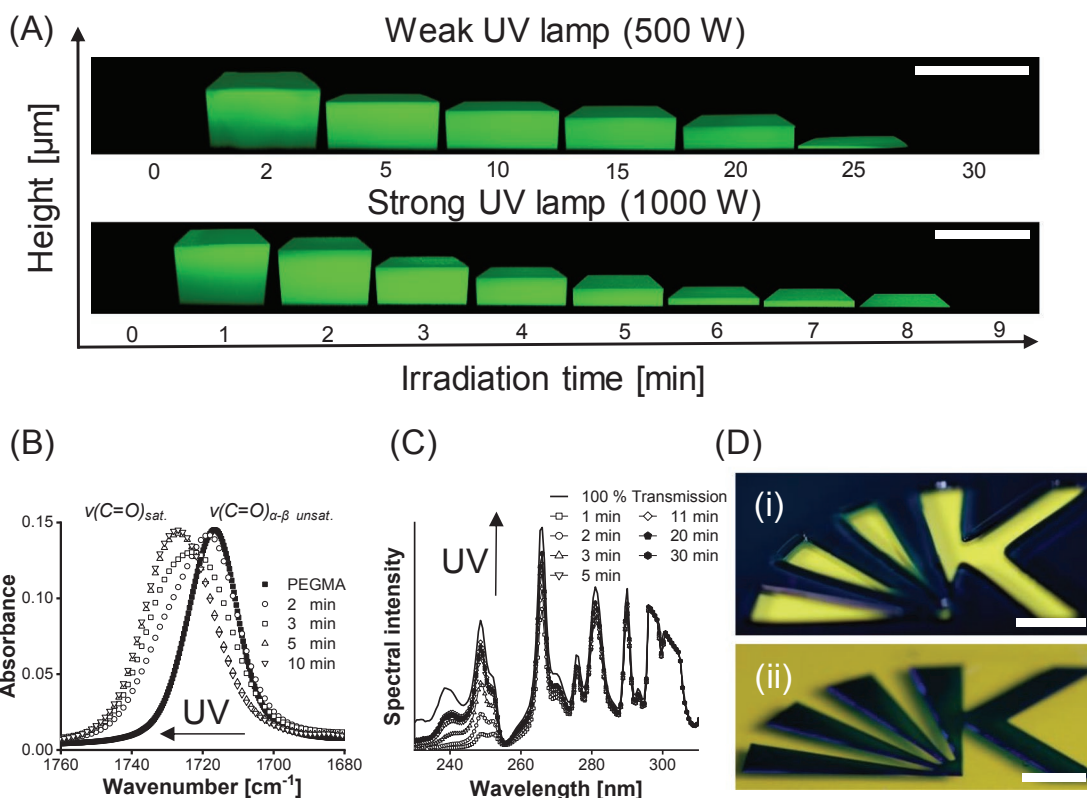


**Figure 3.** A) Visualization of the lifetime of the UV transient hydrogels with confocal microscopy (z-stack images). The hydrogel height is plotted against the irradiation time. Scalebars are 550  $\mu\text{m}$ , the scanned  $x$ - $y$  plane surface area is 0.3025  $\text{mm}^2$ . PEGMA-PEGDMA-5 hydrogel films were prepared for various irradiation times with two different UV lamps (labeled as “strong” and “weak,” see Figures S1–S3, Supporting Information for detailed information). B) Inset on the carbonyl stretching band in ATR FTIR spectra of PEGMA-PEGDMA-5 hydrogel films and PEGMA monomer (normalized). A shift of the peak maximum from 1716  $\text{cm}^{-1}$  of PEGMA (line, normalized to highest gel carbonyl peak) to 1727  $\text{cm}^{-1}$  was observed upon irradiation, indicating the conversion of monomers from unsaturated esters to saturated esters. C) In situ transmission UV spectra showed an increase in UV light transmission over the course of the gelation and liquefaction process. The 100% transmission spectrum shows the UV lamp emission (OAI Model 30). The increase in transmission with increasing irradiation time, particularly between 240 and 290 nm, was attributed to monomer and photoinitiator conversion. D) Inverse PEGMA-PEGDMA-5 hydrogel patterns (blue) prepared from identical materials: Precursor solution, photomask, and light source. Hydrogels were dyed with 4001 Royal Blue ink from Pelikan (Schindellegi, Switzerland) to improve the visibility of the patterns. In (i) a flat hydrogel film was formed via photopolymerization. Then a photomask was put onto the hydrogel film and irradiation was continued until the exposed hydrogel was eroded (positive photoresist). For (ii) a photopolymerization was conducted with a photomask covering parts of the precursor solution (negative photoresist).

a spectrum was recorded for 30 min. As a 100% transmission reference, a film of water (125  $\mu\text{m}$ ) in between two quartz slides was used, which represented the lamp emission spectrum. Upon irradiation the absorbance between 240 and 300 nm decreased rapidly as response to the conversion of double bonds and scission of photoinitiator molecules. In contrast to the spectra of irradiated I2959 in water, no increase in absorbance at 250 nm was observed. This was attributed to overlaps with disappearing PEGMA and PEGDMA alkene bands and the different chemical nature of terminated I2959 radicals in the precursor solution (e.g., initiated polymer chains) when compared to I2959 in water. After  $\approx 5$  min irradiation time, there was no more change in transmission of the lamp emission peak at 266 nm, further confirming the assumption that the polymerization reaction is finished after  $\approx 5$  min. The spectra of 20 and 30 min irradiation time were essentially identical at 266 nm, showing that the UV absorbance of the hydrogel and the resulting degraded polymer solution is the same around this wavelength. The UV transmission of the lamp emission

peak at 249 nm was observed to go through a maximum after 11 min of irradiation, followed by subsequent decay for all longer irradiation times. This decrease is thus indicative for the photodegradation process.

An inherent advantage of photochemistries is the spatial control over a reaction. In the case of UV transient hydrogels, both the formation and degradation are photochemical processes induced by the same light source. This enables spatial control in both the formation and degradation steps, thus making it possible to achieve both spatial and temporal control at the same time. An example of such unique feature is the formation of inverse hydrogel patterns that can be formed and removed through the UV irradiation, serving as both positive or negative photoresists (or both). The inverse hydrogel patterns were yielded using an identical set of materials (UV lamp, hydrogel precursor solution, photomask) simply by covering the sample with a photomask at different time points (Figure 3D). When the photomask was put on a film of hydrogel precursor solution from the beginning, the negative photoresist image is yielded

upon 2 min of irradiation. Irradiation of a film of hydrogel precursor solution for 2 min and a continuation of the irradiation with the photomask placed on top of the hydrogel film yields the inverse image. This unique behavior is believed to be of interest for designing bifunctional photoresists.

Over the course of the solidification (polymerization) and liquefaction (degradation) process, the mechanical properties of the hydrogel films change according to their state of matter (i.e., liquid vs solid). This was exploited to close a quartz capillary for a defined period of time via continuous UV irradiation (Figure 4A). The UV irradiation time required to reopen the capillary could be precisely tailored by varying the relative crosslinker concentration (Figure 4B). Capillaries (100  $\mu\text{m}$  diameter,  $\approx 3$  cm length) were loaded with PEGMA-PEGDMA-*X* precursor solution ( $X = 4, 5,$  and  $6$ ) and were then irradiated ( $4 \text{ mW cm}^{-2}$  at  $260 \text{ nm}$ ) for defined amounts of times and then connected to a syringe filled with dyed water (blue ink). To ensure reproducible results the light intensity was carefully monitored in the exposed area before every single experiment. A 1 kg cast iron weight was then placed on the syringe flange, which exerted a pressure of  $\approx 0.59$  bar on the hydrogel plug in the syringe (based on the syringe's inner diameter of  $14.5 \text{ mm}$  and the acceleration of gravity being  $9.807 \text{ m s}^{-2}$ ). Without irradiation of the hydrogel precursor solution, water could freely pass through the capillary. Irradiation times from 1 to 6, 1 to 8, or 1 to 11 min for PEGMA-PEGDMA-4, -5, and -6, respectively, resulted in a preprogrammed blockage of the capillary, preventing water from passing through. Higher irradiation times again allowed water to freely pass the capillary (Figure 4A,B). Varying the amount of PEGDMA crosslinker between 4 and 6 mol% thus showed to be an easy and efficient way to tailor the lifetime of the hydrogel and remarkably influence macroscopic properties on the minute scale. The UV transient hydrogel plugs the capillary until it is sufficiently degraded to be released by the water pressure applied. In contrast to known transient supramolecular hydrogels, the lifetime of UV transient hydrogels can be extended simply by stopping the UV exposure, e.g., a capillary blocked with PEGMA-PEGDMA hydrogel will remain blocked until further irradiation is applied. When the process of irradiation was stopped and continued  $\approx 1$  h later, the time for freeing the capillary from hydrogel was increased by typically 1–2 min, which is most likely a result of water evaporation from the hydrogel.

The mechanical properties of UV transient hydrogels in the three different stages of their lifetime, i.e., the precursor solution state, the hydrogel state, and the degraded polymer solution state, were investigated. The rheological behavior changed drastically in between the three stages (Figure 4C–E). For the PEGMA-PEGDMA-5 precursor solution and the respective degraded polymer solution, a non-Newtonian behavior typical for polymer solutions was observed.<sup>[38]</sup> This is indicated by the frequency dependence of both storage and loss moduli as well as a crossing point at increasing frequency. The PEGMA-PEGDMA hydrogel showed no crossing points and negligible dependence of the frequency on the storage and loss moduli, indicating a covalently crosslinked polymeric network. Due to the low amount of crosslinker, PEGMA-PEGDMA-5 hydrogels possessed low storage and loss moduli ( $\approx 10^3$  Pa) in the range of soft poly(ethylene glycol) hydrogels used for cell culture.<sup>[39,40]</sup>

In accordance to our expectation, hydrogels swelled to equilibrium were found to have lower moduli than the respective as-prepared hydrogels and PEGMA-PEGDMA-2.5 hydrogels were found to have lower moduli than PEGMA-PEGDMA-5 hydrogels (Figure S8, Supporting Information).

To distinguish the two liquid stages in more detail, the viscosity of PEGMA-PEGDMA-5 precursor solution and a degraded polymer solution (120 min irradiation) was determined (Figure 4F). For the PEGMA-PEGDMA-5 precursor solution a viscosity of  $3.14 \text{ mPas}$  and for the degraded polymer solution (120 min) a viscosity of  $5.95 \text{ mPas}$  was found. The increase in viscosity was attributed to the degraded polymer chains. Their hydrodynamic radius was determined with DLS (dynamic light scattering) to be a broad multimodal distribution between 5 and 500 nm, explaining their influence on the viscosity (Figure 4G).<sup>[41]</sup>

To further demonstrate the different mechanical properties of UV transient hydrogels in their different stages, we measured the stiction force exerted between a hydrogel and a quartz slide (Figure 4H). PEGMA-PEGDMA-5 hydrogel precursor solution was placed on a glass slide and was then covered with a spacer ( $125 \mu\text{m}$ ) and a quartz slide. Samples were then irradiated for different times (0, 2, and 9 min) and the force required to overcome the stiction between the quartz slide and the sample surface was measured with a precision scale. As a result, we could clearly distinguish between the aggregate states of the UV transient hydrogel, since the solid hydrogel state (2 min irradiation) required a higher force ( $4.2 \text{ N}$ ) to overcome the stiction between the sample and the quartz glass compared with the liquid precursor and degraded solution states ( $0.6$  and  $0.9 \text{ N}$ , respectively). We envision that this is a promising concept for transient and preprogrammed adhesives.

### 3. Conclusions

Herein, we introduced the first example of UV transient hydrogels. These covalently crosslinked hydrogels possess an inherent lifetime under continuous UV irradiation, which was enabled by a simultaneous photopolymerization and photodegradation of poly(PEGMA-*co*-PEGDMA) hydrogels. UV transient hydrogels performed an autonomous liquid–gel–liquid process triggered by a single UV source, going from a precursor solution state through a covalently crosslinked hydrogel state into a liquid polymer solution state. The UV reactivity of the systems was thus uniquely dependent on the irradiation time and the current state of the system. In combination with the spatial control of photochemistry this could be exploited to yield two inverse hydrogel patterns using identical starting materials. We also demonstrated how UV transient hydrogels could be used to seal and release a capillary or to manipulate their stiction toward their surroundings, solely based on irradiation time. The lifetime of UV transient hydrogels could be altered via the UV light intensity (or UV source) and the crosslinker concentration (PEGDMA), which led to precise temporal control of macroscopic properties on the minute scale.

The photoreactions and the mechanical properties of UV transient hydrogels were studied with various methods such as ATR FTIR, in situ UV–vis, NMR, CLSM, viscosimetry, and

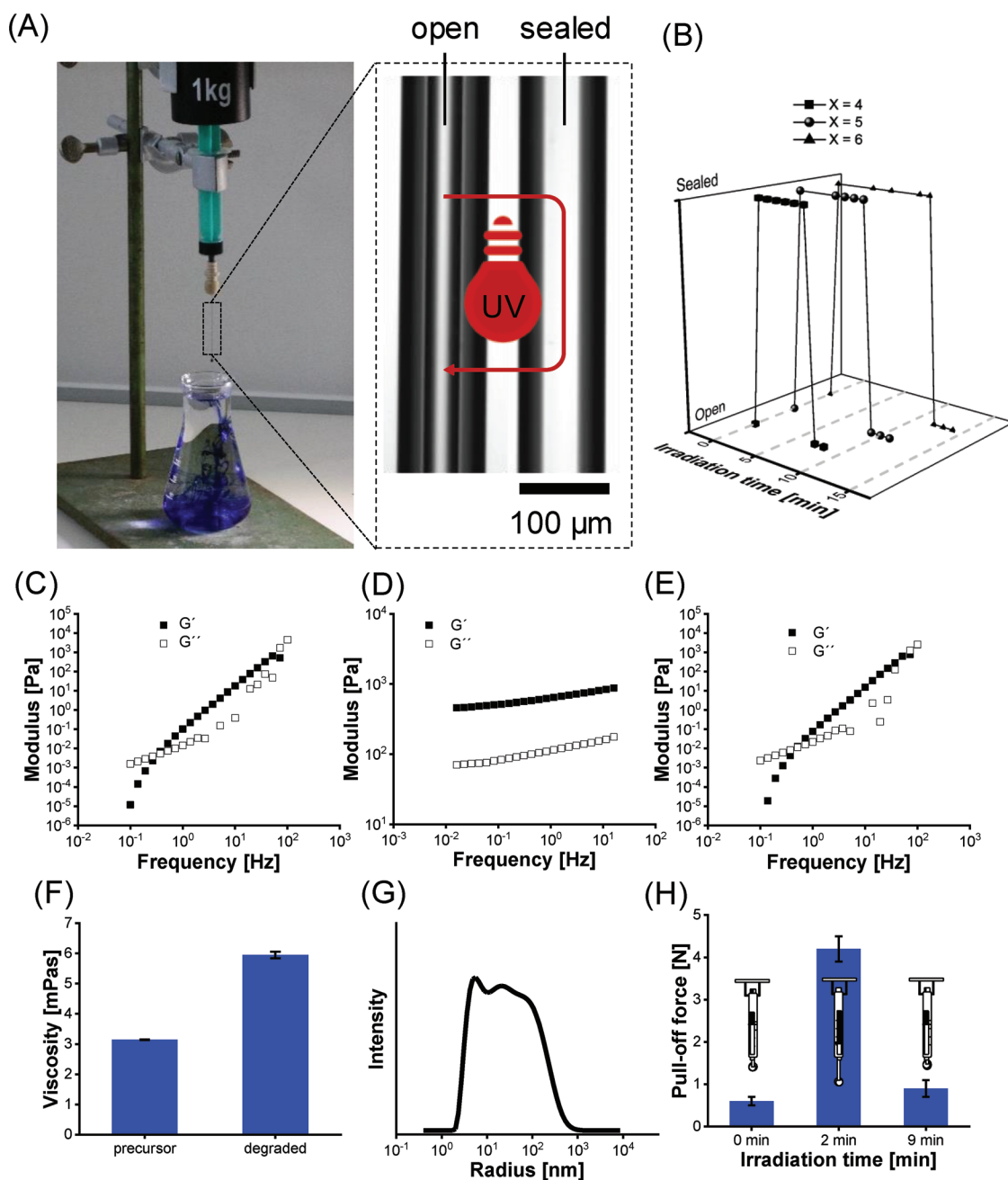


**Figure 4.** A) Irradiation time-dependent sealing of capillaries demonstrating the influence of crosslinker concentration on the lifetimes of UV transient hydrogels. Higher amounts of crosslinker lead to longer irradiation times necessary to open the capillary and enable water flow. A pressure of  $\approx 0.59$  bar was applied to the syringe flange by placing a 1 kg cast iron weight on the plunger flange. The dotted frames show light micrographs of an empty capillary (left) and a capillary with hydrogel photopolymerized inside (right). B) Dependence between irradiation time and the open/sealed state of capillaries infused with PEGMA-PEGDMA- $X$  ( $X = 4, 5, 6$ ) precursor solution. C–E) Comparison of the rheological behavior of PEGMA-PEGDMA-5 precursor solution, hydrogel and degraded polymer solution, respectively. The degraded polymer solution was obtained from irradiation (UVAcube 2000) of PEGMA-PEGDMA-5 hydrogel precursor solution for 120 min in a quartz NMR tube. F) Viscosity of PEGMA-PEGDMA-5 precursor solution and degraded polymer solution, respectively. The degraded polymer solution was obtained from irradiation (UVAcube 2000) of PEGMA-PEGDMA-5 hydrogel precursor solution for 120 min in a quartz NMR tube. G) DLS (dynamic light scattering) measurement of degraded polymer solution obtained from irradiation (UVAcube 2000) PEGMA-PEGDMA-5 hydrogel precursor solution for 120 min in a quartz NMR tube. H) Pull-off force required to remove a quartz glass slide from the surface of PEGMA-PEGDMA-5 films after different irradiation times (UVAcube 2000).

rheometry. Irradiation time-dependent photoreactive systems could be interesting materials for applications as advanced photoresists since the same precursor solution can be used as

both positive and negative photoresist. Further, this principle could be applied to adhesives, where a targeted application and on-demand removal are of great interest. It is believed that a

transfer of this general concept to less energetic wavelengths bears potential in areas such as targeted medicine or cell biology (e.g., cell encapsulation and release).

## Supporting Information

Supporting Information is available from the Wiley Online Library or from the author.

## Acknowledgements

This work was supported by the European Research Council (ERC) Starting Grant (ID: 337077-DropCellArray), Helmholtz Association's Initiative and Networking Fund (Grant No. VH-NG-621). The authors thank Maxi Hoffmann and Lukas Arens for help with rheology measurements and Stefan Heissler for help with the ATR FTIR measurements. J.S. acknowledges the DBU for financial support.

## Conflict of Interest

The authors declare no conflict of interest.

## Keywords

hydrogels, photodegradation, photopolymerization, preprogrammed, transient

Received: November 24, 2019  
Revised: December 16, 2019  
Published online: January 9, 2020

- [1] W. Lee, H. Lee, J. Cha, T. Chang, K. J. Hanley, T. P. Lodge, *Macromolecules* **2000**, *33*, 5111.
- [2] T. S. Fischer, D. Schulze-Sünninghausen, B. Luy, O. Altintas, C. Barner-Kowollik, *Angew. Chem., Int. Ed.* **2016**, *55*, 11276.
- [3] J.-F. Lutz, M. Ouchi, D. R. Liu, M. Sawamoto, *Science* **2013**, *341*, 1238149.
- [4] L. Barner, T. P. Davis, M. H. Stenzel, C. Barner-Kowollik, *Macromol. Rapid Commun.* **2007**, *28*, 539.
- [5] P. J. M. Stals, Y. Li, J. Burdyńska, R. Nicolay, A. Nese, A. R. A. Palmans, E. W. Meijer, K. Matyjaszewski, S. S. Sheiko, *J. Am. Chem. Soc.* **2013**, *135*, 11421.
- [6] Y. Hao, E. W. Fowler, X. Jia, *Polym. Int.* **2017**, *66*, 1787.
- [7] I. M. El-Sherbiny, M. H. Yacoub, *Global Cardiol. Sci. Pract.* **2013**, *2013*, 316.
- [8] E. Caló, V. V. Khutoryanskiy, *Eur. Polym. J.* **2015**, *65*, 252.
- [9] J. H. van Esch, R. Klajn, S. Otto, *Chem. Soc. Rev.* **2017**, *46*, 5474.
- [10] A. Sorrenti, J. Leira-Iglesias, A. Sato, T. M. Hermans, *Nat. Commun.* **2017**, *8*, 15899.
- [11] L. Heinen, T. Heuser, A. Steinschulte, A. Walther, *Nano Lett.* **2017**, *17*, 4989.
- [12] D. Spitzer, L. L. Rodrigues, D. Straßburger, M. Mezger, P. Besenius, *Angew. Chem., Int. Ed.* **2017**, *56*, 15461.
- [13] E. Jee, T. Bánsági, A. F. Taylor, J. A. Pojman, *Angew. Chem.* **2016**, *128*, 2167.
- [14] T. Heuser, E. Weyandt, A. Walther, *Angew. Chem.* **2015**, *127*, 13456.
- [15] J. P. Wojciechowski, A. D. Martin, P. Thordarson, *J. Am. Chem. Soc.* **2018**, *140*, 2869.
- [16] J. Boekhoven, W. E. Hendriksen, G. J. M. Koper, R. Eelkema, J. H. van Esch, *Science* **2015**, *349*, 1075.
- [17] L. Heinen, A. Walther, *Soft Matter* **2015**, *11*, 7857.
- [18] B. Zhang, I. M. Jayalath, J. Ke, J. L. Sparks, C. S. Hartley, D. Konkolewicz, *Chem. Commun.* **2019**, *55*, 2086.
- [19] E. A. Appel, J. del Barrio, X. J. Loh, O. A. Scherman, *Chem. Soc. Rev.* **2012**, *41*, 6195.
- [20] X. Du, J. Zhou, J. Shi, B. Xu, *Chem. Rev.* **2015**, *115*, 13165.
- [21] B. D. Fairbanks, M. P. Schwartz, C. N. Bowman, K. S. Anseth, *Biomaterials* **2009**, *30*, 6702.
- [22] S. Smolne, S. Weber, M. Buback, *Macromol. Chem. Phys.* **2016**, *217*, 2391.
- [23] A. G. Evans, E. Tyrrell, *J. Polym. Sci.* **1947**, *2*, 387.
- [24] T. Çaykara, O. Güven, *Polym. Degrad. Stab.* **1999**, *65*, 225.
- [25] O. Chiantore, L. Trossarelli, M. Lazzari, *Polymer* **2000**, *41*, 1657.
- [26] R. W. Johnstone, I. G. Foulds, M. Parameswaran, *J. Vac. Sci. Technol., B* **2008**, *26*, 682.
- [27] H. Kaczmarek, A. Kamińska, A. van Herk, *Eur. Polym. J.* **2000**, *36*, 767.
- [28] T. Mitsuoka, A. Torikai, K. Fueki, *J. Appl. Polym. Sci.* **1993**, *47*, 1027.
- [29] R. Shanti, A. N. Hadi, Y. S. Salim, S. Y. Chee, S. Ramesh, K. Ramesh, *RSC Adv.* **2017**, *7*, 112.
- [30] A. R. Shultz, *J. Phys. Chem.* **1961**, *65*, 967.
- [31] A. Torikai, M. Ohno, K. Fueki, *J. Appl. Polym. Sci.* **1990**, *41*, 1023.
- [32] C. Wochnowski, M. A. Shams Eldin, S. Metev, *Polym. Degrad. Stab.* **2005**, *89*, 252.
- [33] C. D. O'Connell, B. Zhang, C. Onofrillo, S. Duchi, R. Blanchard, A. Quigley, J. Bourke, S. Gambhir, R. Kapsa, C. Di Bella, P. Choong, G. G. Wallace, *Soft Matter* **2018**, *14*, 2142.
- [34] M. Liu, M.-D. Li, J. Xue, D. L. Phillips, *J. Phys. Chem. A* **2014**, *118*, 8701.
- [35] L. Li, J. M. Scheiger, T. Tronser, C. Long, K. Demir, C. L. Wilson, M. A. Kuzina, P. A. Levkin, *Adv. Funct. Mater.* **2019**, *29*, 1902906.
- [36] Y. S. Kim, C. S. P. Sung, *J. Appl. Polym. Sci.* **1995**, *57*, 363.
- [37] X.-S. Chai, F. J. Schork, E. M. Oliver, *J. Appl. Polym. Sci.* **2006**, *99*, 1471.
- [38] P. J. Carreau, D. D. Kee, M. Daroux, *Can. J. Chem. Eng.* **1979**, *57*, 135.
- [39] A. M. Jonker, S. A. Bode, A. H. Kusters, J. C. M. van Hest, D. W. P. M. Löwik, *Macromol. Biosci.* **2015**, *15*, 1338.
- [40] F.-C. Chang, C.-T. Tsao, A. Lin, M. Zhang, S. L. Levengood, M. Zhang, *Polymers* **2016**, *8*, 112.
- [41] N. Kang, Y. J. Zuo, L. Hilliou, M. Ashokkumar, Y. Hemar, *Food Hydrocolloids* **2016**, *52*, 183.